The Effects of Temporal Sampling and Changing Spatial Scales on the Mapping of Forest Cover in Yellowstone National Park Using Imaging Spectroscopy

Raymond F. Kokaly,* Roger N. Clark,* Don G. Despain,** and K. Eric Livo*

* U.S. Geological Survey, MS 973, Box 25046, Federal Center, Denver, Colorado 80225
** U.S. Geological Survey-Biologic Resources Division, Bozeman, Montana

1. INTRODUCTION

The U.S. Geological Survey (USGS), in cooperation with the National Park Service, is using imaging spectroscopy to advance the understanding of the geologic features and biologic systems in Yellowstone National Park. Kokaly et al. (1998 and 2001) presented the methods and results of applying imaging spectroscopy to the study of the biotic components of Yellowstone National Park. Knowledge of the distribution of vegetation such as whitebark pine is desired for understanding the habitat and movements of grizzly bears, bison and other large mammals. This paper addresses several questions regarding the mapping of forest cover in Yellowstone National Park (Yellowstone) using imaging spectroscopy, including:

1) How do the spectral signatures of conifer forest stands differ when changing the spatial scale and temporal sampling of Airborne Visible and Infrared Imaging Spectrometer (AVIRIS) data?
2) Can conifer forest cover types be robustly identified in high spatial resolution AVIRIS data using the USGS Tetracorder system and a vegetation spectral library derived from a lower spatial resolution data set?
3) How do maps of forest cover derived from low and high spatial resolution AVIRIS data compare?

2. BACKGROUND

2.1 Yellowstone Forest Cover

Most of Yellowstone is covered by forests which can be divided into four major conifer cover types: lodgepole pine (*Pinus contorta*), whitebark pine (*Pinus albicaulis*), Douglas-fir (*Pseudotsuga menziesii*), and mixed Engelmann Spruce/Subalpine Fir (*Picea engelmannii/Abies lasiocarpa*). As a result of fire history and soil conditions, the current dominant forest cover in Yellowstone is lodgepole pine. The temperate forests at high elevations in the park receive much moisture during the long, cold winter. According to Despain (1990), the mean duration of snow cover is about 271 days at 9,000 feet elevation. At lower elevations, in Yellowstone's relatively drier valleys, dry grasslands and sagebrush steppe communities dominate. The geology underlying the vegetation in Yellowstone has an influence on the distribution of plants within the park (Despain, 1990). In areas with andesitic rocks, the higher nutrient content supports climax forests of mixed Engelmann spruce/subalpine fir. Douglas-fir occurs in moisture rich areas of

the park such as north-facing slopes. Soils derived from rhyolite flows within the park have relatively low nutrient content; in these areas, the dominant forest type is lodgepole pine

2.2 Imaging Spectroscopy of Forests and Remote Sensing of Yellowstone

Airborne imaging spectroscopy has been shown to have the ability to discriminate different vegetation types from one another. Clark et al. (1995a) used AVIRIS data to accurately map the distributions of various agricultural crops in the San Luis Valley of Colorado. Natural forest types in an area of deciduous, mixed deciduous/conifer, and conifer cover have also been differentiated (Martin et al., 1998). Imaging spectroscopy has also been studied for the possibility of determining canopy nitrogen concentrations (Wessman et al., 1989; Martin and Aber, 1997; Kokaly and Clark, 1999). Ustin et al. (1999) reviewed the role of remote sensing in linking biologic observations to geologic studies in their discussion of geobotanical studies. Roberts et al. (1998) used airborne spectrometer data combined with spectral mixture modeling to map the distribution of different chaparral vegetation types in the Santa Monica Mountains.

In Yellowstone National Park (Yellowstone), Despain (1990) used aerial photography to make vegetation maps. These maps include the distribution of the four major forest types and various age classes of lodgepole pine. Jakubauskas (1996) used Landsat TM data in an attempt to map the distribution of forest cover types in Yellowstone. Kokaly et al. (1998 and 2001) used AVIRIS data over several areas of Yellowstone to map the distribution of forest cover types, nonforest cover types, and surface microbial mats. This study used the USGS Tetracorder system applied to AVIRIS data obtained on the high altitude platform (an ER-2 aircraft collecting data at approximately 17 meter pixel size). In particular, this study was effective at identifying the occurrence of whitebark pine using a comparison of the shapes of vegetation chlorophyll and water absorption features (Kokaly et al., 2001).

3. METHODS

3.1 AVIRIS Data Collection and Calibration

The AVIRIS instrument was flown over Yellowstone in 1996 and 1998. The 1996 AVIRIS data, hereafter referred to as the high altitude data, was acquired using the NASA ER-2 aircraft at 65,000 ft altitude. The 1998 AVIRIS data, hereafter referred to as the low altitude data, was acquired using a Twin Otter aircraft flying at approximately 12,000 ft altitude. For this paper, an area of lodgepole forest near Old Faithful Geyser was selected to compare reflectance spectra and mapping results between these two data sets. Table 1 summarizes the data collection parameters for this study site. In particular, note the low solar elevation for the low altitude data (34^{o}).

In order to convert AVIRIS data from radiance to reflectance, the data had to be corrected for the influence of several variables, including solar irradiance, atmospheric gas absorptions, and path radiance. A two-step procedure for this conversion, as described by Clark et al. (1993a, 1995b, and 2001a), was employed, which includes: 1) primary atmospheric correction using the ATREM algorithm (Gao et al., 1993 and 1997), and 2) correction of residual features using ground calibration.

For both AVIRIS data acquisitions, a ground calibration site was selected by field survey as having the properties of being fairly large, homogenous, and not containing material with strong absorption features. A gravel staging area, located near Norris Geyser Basin, was utilized for

calibration of high altitude data. On the day of the AVIRIS flight, reflectance measurements of this site were made with a field spectrometer having the same spectral coverage as the AVIRIS instrument. Spectra of the calibration site, extracted from the ATREM-corrected AVIRIS data, were used with the field measurements to generate a multiplicative correction. An additive path radiance correction was derived using an area of vegetation in shadow. Following the initial correction using ATREM, these additive and multiplicative corrections were applied to each pixel of AVIRIS data to derive surface reflectance. For more specific information on the calibration of the high altitude data see Kokaly et al. (2001).

The low altitude data were calibrated using field reflectance spectra of the large parking lot near Old Faithful Geyser. The procedure for reflectance calibration of the data was similar to that of the high altitude data, including the use of the darkest, shaded vegetation pixels for path radiance correction. The low altitude data were sampled at 1.5 meters in the cross-track direction and 4.3 meters in the along track direction. The data were corrected for aircraft motions and resampled using nearest-neighbor methods to give a rectified image (Boardman, 1999).

3.2 Spectral Feature Analysis

In order to compare the shapes of the absorption features between samples, this study used a method of normalization called continuum removal. Continuum removal, or baseline normalization, is a method commonly used in laboratory infrared spectroscopy (Ingle, 1988). Clark and Roush (1984) discussed the application of this method to remotely-sensed reflectance spectra. Clark et al. (1990) first applied this method to terrestrial imaging spectrometer data to map the distribution of minerals and vegetation by comparing remotely sensed absorption band shapes to those in a reference spectral library. Continuum removal is a numerical method to estimate the absorptions not due to the band of interest and remove their effects and to eliminate reflectance level changes due to view and illumination geometry variations (Clark and Roush, 1984; Clark, 1999).

Figure 1 shows the continuum removed chlorophyll absorption feature of the Yellowstone forest cover types. The depth of the chlorophyll absorption feature is affected by the concentration of chlorophyll in the forest canopy, the percent cover of the forest canopy, the understory vegetation, and soil background. In addition, multiple scattering effects can also affect the apparent strength of the chlorophyll absorption feature. In Figure 1, the pines show weaker absorption strengths with lodgepole pine (LP) having the weakest chlorophyll absorption. Douglas-fir (DF) has the strongest absorption feature. Continuum removed absorption features of plants have been compared by scaling them to the same depth at the band center, thus, allowing a comparison of the shapes of absorption features (see Kokaly and Clark, 1999).

3.3 USGS Tetracorder Expert System

In this study, the USGS Tetracorder system was applied to AVIRIS data over Yellowstone to differentiate between vegetation cover types. The USGS Tetracorder system has been used to identify and map distributions of minerals and vegetation in AVIRIS data (Clark et al., 1990, 1991, 1993b, 1995c, and 2001b). Tetracorder is an expert system that can compare the characteristic absorption features of materials assembled in a spectral library to the absorption features present in the spectrum of each pixel of AVIRIS data. Tetracorder uses continuum removal to isolate specific absorptions and remove the effects of changing slopes and overall reflectance levels (Clark and Roush, 1984). Tetracorder compares the wavelength position and

shape of absorption features in the reference spectra of entries in the library with those in the AVIRIS data. A modified least-squares fitting algorithm is used to assess the closeness of the match (Clark et al., 1990). The Tetracorder expert system makes further refinements to select the closest match using threshold values, continuum slope constraints and other methods (Clark et al., 2001b).

The development of a spectral library of vegetation reflectance was an integral part of vegetation cover mapping in Yellowstone National Park (see Kokaly et al., 2001). The major cover types in Yellowstone NP were identified during a field survey. These cover types included all significant forest cover types, including lodgepole pine (LP), whitebark pine (WB), Douglas-fir (DF), and a mixed Engelmann spruce/subalpine fir category (SF). To define spectral signatures of these vegetation types, pixels in the AVIRIS data covering these vegetation types were averaged together to generate representative spectra. Nearly 40 such training sites were identified in the AVIRIS data. To illustrate the comparison of spectral features by Tetracorder, the reflectance spectrum of a single pixel of AVIRIS data was compared to the entries of this spectral library. Figure 2 shows how the continuum removed chlorophyll absorption features compare between the pixel and the closest match identified by the USGS Tetracorder system (lodgepole pine).

4. SPECTRAL COMPARISONS

4.1 Observations in Low Altitude AVIRIS Reflectance Data

The low altitude AVIRIS data with its small pixel size and lower sun angle showed variations in reflectance level based on local slope of the surface. For example, Figure 3 shows the change in reflectance level between the two pitched sides of the roof of a visitor's lodge in the Old Faithful area. The reflectance level at 1.7 μm for the south facing side is over 4.5 times higher than the dark north-facing slope of the roof. Thus, algorithms applied to this data set must be insensitive to these reflectance level variations. The continuum removal process used in the USGS Tetracorder system is an example of one type of normalization procedure that compensates for reflectance level. Algorithms such as linear unmixing will be sensitive to this change and increase the fraction of the compensatory "shade" endmember. Thus, linear unmixing of the sunlit vs. shaded side of the roof will yield different coverage fractions. As a result, this simple situation shows that the fraction values yielded by linear unmixing do not represent physical fractions of areal coverage.

This simple observation of reflectance level changes based on local slope of a surface led to an investigation of the more complex situation encountered in a forest stand. The low altitude data had a pixel size of 1.5 meters. In a forest, this allows resolution of a variety of surfaces, including: sunlit and shaded tree crowns and sunlit and shaded understory vegetation. The reflectance spectrum of a single pixel of the low altitude AVIRIS data results from one or more of these components. A simple example of these effects was examined in the parking lot of Old Faithful. The reflectance spectra of lodgepole trees in the parking lot, shaded trees, shaded asphalt and sunlit asphalt are shown in Figure 4. The reflectance variations show a complication in the shaded pixels. The reflectance of shaded parking lot pixels shows an artificial increase toward the short wavelengths. It is suggested that this effect is primarily due to an inaccurate calculation of true reflectance by an insufficient estimation of the diffuse sky irradiance of the surface. ATREM assumes a standard ratio of diffuse:direct irradiance for every pixel. Mustard

et al. (1999) observed ATREM's inability to give reflectance curves over the ocean surface. Mustard et al. (1999) used cloud shadows to estimate atmospheric path radiance correction and used the assumption of a constant multiplicative factor to compensate for diffuse sky irradiance. Gao et al. (1993) noted several limitations and possible error sources for ATREM, including: hazy conditions, assumption of a mean elevation and orientation for the entire scene, assumption of nadir view angle only, and atmospheric and topographic adjacency effects.

A more complicated method of estimating the diffuse:direct irradiance on a pixel by pixel basis is required to derive true surface reflectance for each pixel. The assumption of a constant sky irradiance correction factor used by Mustard et al. (1999) for correcting AVIRIS data over water is not applicable in this situation because terrestrial surfaces have variable slopes and land surface elements cast shadows. The use of a Digital Elevation Model (DEM) will allow the correction for topographic variation. However, local slope changes such as the roof slope in Figure 3, the shaded parking lot in Figure 4, or the orientation and illumination of tree crowns is a much more difficult problem to correct. Thus, if such corrections are not feasible, analysis algorithms must be able to deal with these complicated effects on reflectance spectra due to changing illumination conditions.

4.2 Reflectance from a Lodgepole Pine Stand in Low Altitude AVIRIS Data

The situation of shading caused by trees in the simple example in the Old Faithful parking lot becomes much more complicated in the midst of a stand of conifer trees. Figure 5 shows the variation in spectra of low altitude data for a stand of lodgepole pine located just north of the Old Faithful Geyser. The range in reflectance level and the spectral shapes are quite high. This pixel-to-pixel variation is attributed to the measurement of sunlit and shaded tree crowns and understory vegetation, as well as multiple scattering effects. In addition, shaded pixels show an increase in reflectance toward the short wavelengths similar to that observed for shaded pixels in the Old Faithful parking lot. Thus, the shaded forest pixels have not been converted to true reflectance. Therefore, care must be taken in interpreting the spectra from these pixels.

In order to assess the change in spectra from high spatial resolution (1.5 m) to low spatial resolution (~17.5 m), 12x12 pixel areas of the low altitude data were averaged to approximate the pixel size of the high altitude data. The resulting variations in reflectance between averaged areas (Figure 6) are less than the variations for single pixels (Figure 5). Note that the averaged pixels still contain the influence of shaded pixels that have not been corrected to true reflectance.

4.3 Comparisons of Lodgepole Reflectance between High and Low Altitude AVIRIS Data

To assess the changes in reflectance for conifer forests between high and low altitude AVIRIS data, the pixels covering an area of lodgepole pine forest north of Old Faithful were averaged for the high altitude and low altitude data sets. Figure 7a shows the comparison of low altitude and high altitude average reflectance spectra. The curves show similar spectral shape but an offset in overall reflectance level. There are several influences that may cause this change in the level, including: differences in illumination and viewing geometry and changes in overstory and understory vegetation state. The geometrical considerations act to lower the reflectance of the low altitude data as observed. The lower sun angle of the low altitude data contributes to a higher degree of shading which lowers the overall reflectance level of the forest stand. Changes in understory vegetation are another factor; a comparison of the reflectance from adjacent meadows shows that the grasses have senesced more in the October low altitude data set compared to the August high altitude data set. The influence of the change in understory would

be to increase the reflectance level due to decreased absorption by chlorophyll and water in the nonforest vegetation. However, as Figure 7a shows, the changing illumination has a stronger influence than the background vegetation in the lodgepole pine stand and the October data has a lower reflectance level than the August data.

A comparison of the chlorophyll absorption feature at 0.68 μm after continuum removal and normalization to the band depth showed a high level of comparison (Figure 8b). Using the modified least-squares approach of Clark et al. (1990), the correlation fit number (which ranges from 0, no correlation, to 1, an exact correlation) between the two spectra was 0.999. Thus, despite the changing reflectance level due to differing sun-surface-sensor geometry between the measurements and the change in vegetation state from the August 1996 to the October 1998 data collections, the average spectra of the lodgepole pine stand were remarkably similar in shape. In particular, continuum removal and normalization to the band center showed that the chlorophyll feature has changed very little between measurements (Figure 7b). There is a slight blue-shift of the red-edge in the high altitude spectrum as compared to the low altitude spectrum. The effects of changing illumination conditions and vegetation state influence the position of the red edge.

5. MAPPING RESULTS

In order to test the forest cover mapping method developed for the high altitude 1996 AVIRIS data by Kokaly et al. (2001), the same procedure used in that study was applied to the low altitude 1998 AVIRIS data for a scene covering the Old Faithful geyser area. Specifically, the USGS Tetracorder system was used to compare the reflectance spectrum of each pixel of the low altitude AVIRIS scene to the entries in the spectral library of vegetation cover types. This library of vegetation cover types was derived from the high altitude data set by extracting and averaging pixels over known vegetation cover types. Kokaly et al. (2001) used the USGS Tetracorder system applied to the 0.68 μm chlorophyll feature and the 0.98 μm and 1.20 μm water absorption features observed in vegetation canopy reflectance.

The results of the high altitude study for the Old Faithful area are presented in Figure 8. The vegetation in this area was identified as dominantly lodgepole pine. However, scattered pixels of the other conifers are found in a noisy pattern throughout the scene. While the majority of pixels in the high altitude data mapped as lodgepole pine, some mapped as whitebark pine. Fewer numbers of pixels are mapped as Douglas-fir. Finally the least number of pixels in the high altitude data are mapped as Engelmann spruce/Subalpine fir.

The results of the low altitude mapping of forest cover types are shown in Figure 9. Again, the dominant cover type mapped is lodgepole pine. The pixels that map as forest cover are mainly the brightly-lit tree crowns of the forest stand. Note that the shadow pixels in the lodgepole forest stand in Figure 9 are not identified as any of the forest cover types. The reasons for this are suggested as follows: 1) the shadow pixels are mainly shaded nonforest vegetation, 2) the reflectance levels of the shaded pixels are very low, and 3) the atmospheric correction procedure is inaccurate for the shaded pixels which have a high degree of diffuse illumination relative to direct solar illumination and, therefore, spectra of these pixels do not represent the true reflectance of the surface.

Figure 10 shows a subset of the high altitude forest cover map for comparison to the low altitude cover map in Figure 9. There is generally good agreement in mapping most of the area as lodgepole pine cover. The low altitude data with its smaller pixel size shows a slightly

different distribution of lodgepole. In particular, the low altitude data resolve individual trees within the lodgepole stand and show the gaps between trees. The low altitude data also show the occurrence of just a few trees in some areas (e.g., the parking lot of the Old Faithful area). In comparison, the high altitude data show the forest stands as being near contiguous pixels of conifer cover. In this study, the ability of the high altitude data to estimate the variability in density of trees was not explored. Also, small stands or single trees mapped in the low altitude data were not detected in the high altitude data (e.g., note the developed areas south of Old Faithful geyser). The fact that the tree crowns of lodgepole pine are mapped in the low altitude data using average reflectance signatures from the high altitude data suggests that the conifer reflectance at the 17.5 meter scale is dominated by the reflectance from the individual trees.

6. CONCLUSIONS

This study of the differences in mapping forest cover with high altitude August 1996 AVIRIS data and low altitude October 1998 AVIRIS data was conducted to understand reflectance changes between spectral data with different seasonal sampling and spatial resolution. Furthermore, the forest cover mapping method of Kokaly et al. (2001) was tested for robust application between the data sets. The results of the study showed that the low altitude data set, with its low sun angle and small pixel size, showed greater variation in reflectance level due to local slope and the orientation of surfaces such as tree crowns. In addition, for pixels in shadow true reflectance was not calculated by the atmospheric correction procedure because the correct proportion of diffuse:direct illumination was not specified on a pixel by pixel basis. The observed error in surface reflectance retrievals due to diffuse:direct irradiance is dependent on solar zenith angle, sky conditions (e.g., cloudiness), local slope of the surface, and the orientation of elements such as tree crowns. The high altitude data with 17.5 meter pixel size does not contain a single pixel that is fully shadowed. However, the reflectance of forests as measured from the high altitude data also had the influence of incorrect calculation of true reflectance due to inadequate specification of the diffuse:direct reflectance for shaded parts of the canopy and understory.

An examination of the reflectance changes through a stand of lodgepole pine in the Old Faithful area showed the pixel to pixel variations to be much greater at the 1.5 meter scale compared to 17.5 meter pixels. The variations are due to sunlit vs. shaded tree crowns and understory. It is also suggested that multiple scattering between canopy elements affects the shape of the spectra. Reflectance observed for forest pixels, from the high altitude data, are likely a combination of reflectance from individual surface elements that have not been compensated for nonlinear effects (e.g. multiple scattering, sunlit vs. shaded vegetation). These nonlinear effects were observed in low altitude data. It was observed that the reflectance of deeply shaded forest areas was affected by insufficient correction for illumination conditions, which altered the spectral shapes. Thus, in some shadowed pixels the identification of vegetation cover type was compromised.

A comparison of the average reflectance for a stand of lodgepole pine between the high altitude and low altitude AVIRIS data showed a higher reflectance level in the high altitude data. The reflectance level of the low altitude data is suggested to be lower due to the low sun angle and a greater proportion of shadowed vegetation in the forest stand. However, continuum removal and normalization to band depth of the 0.68 μm chlorophyll absorption feature show

very little variation between the two data sets. This suggests that, despite the limitations of the combined radiative transfer and ground calibration method of atmospheric correction employed here, the forests in Yellowstone have consistent spectral absorption features that may be used for consistent and repeatable mapping of forest cover types.

The possibility of developing a robust vegetation cover mapping method for the Yellowstone area was tested by mapping the distribution of forest cover types in the low altitude 1998 AVIRIS data using the USGS Tetracorder system and a spectral library of vegetation cover types derived from the high altitude 1996 AVIRIS data. The USGS Tetracorder system successfully handled the change in spatial scale and timing of AVIRIS data collection to reproduce maps of forest cover in the Old Faithful area of Yellowstone National Park. Indeed, the increased spatial resolution of the low altitude data enables improved mapping of the forest structure by detecting tree crowns, gaps, and individual trees. Further analysis of such low altitude data may lead to the development of tree counts or tree density estimates using this detection of crowns and gaps. Bi-directional reflectance distribution function effects were observed but did not cause a problem for identifying conifer species using the USGS Tetracorder system, in part because the system isolates absorption features using continuum removal. Additional work should be conducted on other imaging spectroscopy data sets for Yellowstone National Park, such as high altitude 1997 AVIRIS data. In addition, further studies in more diverse areas of forest cover are needed in order to develop a robust method of mapping conifers using spectral feature analysis and imaging spectrometer data.

7. REFERENCES

Boardman, J.W. (1999) "Precision geocoding of low altitude AVIRIS data: Lessons learned in 1998," *Summaries of the 8th JPL Airborne Earth Science Workshop*, R.O. Green, Ed., JPL Publication 99-17, pp. 63-68.

Clark, R.N., G.A. Swayze, T.V.V. King, K.E. Livo, R.F. Kokaly, J.B. Dalton, J.S. Vance, B.W. Rockwell, and R. R. McDougal (2001a) "Surface Reflectance Calibration of Terrestrial Imaging Spectroscopy Data: a Tutorial Using AVIRIS," Draft of U.S. Geological Survey Open File Report, available online at: http://speclab.cr.usgs.gov/PAPERS.calibration.tutorial/calibntA.html

Clark, R.N., Swayze, G.A., and King, T.V.V. (2001b) "Imaging Spectroscopy: A Tool for Earth and Planetary System Science Remote Sensing with the USGS Tetracorder System," submitted to *Journal of Geophysical Research*.

Clark, R.N. (1999), Spectroscopy of rocks and minerals and principles of spectroscopy. In *Remote Sensing for the Earth Sciences: Manual of Remote Sensing 3rd Edition, Vol. 3* (A.N. Rencz Ed.), John Wiley and Sons, Inc., New York, pp. 3-58.

Clark, R.N., T.V.V. King, C. Ager, and Swayze, G.A. (1995a) "Initial vegetation species and senescence/stress indicator mapping in the San Luis Valley, Colorado using imaging spectrometer data," *Summaries of the Fifth Annual JPL Airborne Earth Science Workshop*, January 23- 26, 1995, R.O. Green, Ed., JPL Publication 95-1, p. 35-38.

Clark, R.N., G.A. Swayze, Heiebrecht, K.B., Green, R.O., and Goetz, A.F.H. (1995b) "Calibration to Surface Reflectance of Terrestrial Imaging Spectrometry Data: Comparison of Methods," *Summaries of the Fifth Annual JPL Airborne Earth Science Workshop*, January 23- 26, 1995, R.O. Green, Ed., JPL Publication 95-1, pp. 41-42.

Clark, R.N. and Swayze, G.A. (1995c) "Mapping Minerals, Amorphous Materials, Environmental Materials, Vegetation, Water, Ice and Snow, and Other Materials: The USGS Tricorder Algorithm," *Summaries of the Fifth Annual JPL Airborne Earth Science Workshop,* January 23- 26, R.O. Green, Ed., JPL Publication 95-1, p. 39-40.

Clark, R.N., G.A. Swayze, Heiebrecht, K.B., Goetz, A.F.H, and Green, R.O. (1993a) "Comparison of Methods for Calibrating AVIRIS Data to Ground Reflectance," *Summaries of the 4th Annual JPL Airborne Geosciences Workshop, Volume 1: AVIRIS Workshop,* JPL Publication 93-26, pp. 31-34.

Clark, R.N., Swayze, G.A., and Gallagher, A. (1993b) "Mapping Minerals with Imaging Spectroscopy," *U.S. Geological Survey, Office of Mineral Resources Bulletin 2039,* pp. 141-150.

Clark, R.N., G.A. Swayze, A. Gallagher, N. Gorelick, and F. Kruse (1991) "Mapping with Imaging Spectrometer Data Using the Complete Band Shape Least-Squares Algorithm Simultaneously Fit to Multiple Spectral Features from Multiple Materials," *Proceedings of the Third Airborne Visible/Infrared Imaging Spectrometer (AVIRIS) Workshop,* JPL Publication 91-28, 2-3.

Clark, R.N., A.J. Gallagher, and G.A. Swayze, 1990, "Material Absorption Band Depth Mapping of Imaging Spectrometer Data Using a Complete Band Shape Least-Squares Fit with Library Reference Spectra," *Proceedings of the Second Airborne Visible/Infrared Imaging Spectrometer (AVIRIS) Workshop.* JPL Publication 90-54, 176-186.

Clark, R. N. and T.L. Roush, 1984, "Reflectance Spectroscopy: Quantitative Analysis Techniques for Remote Sensing Applications," *Journal of Geophysical Research,* **89**:6329-6340.

Despain, D. G., 1990, Yellowstone Vegetation: Consequences of Environment and History in a Natural Setting, Roberts Rinehart Publishers, Santa Barbara.

Gao, B.C., Heidebrecht, K.B., and Goetz, A.F.H., 1993, "Derivation of Scaled Surface Reflectances from AVIRIS Data," *Remote Sensing of Environment,* **44**:165-178.

Gao, B.C., Heidebrecht, K.B., and Goetz, A.F.H., 1997, "Atmosphere Removal Program (ATREM) Version 3.0 User's Guide," Center for the Study of Earth from Space, University of Colorado at Boulder, pp. 1-27.

Ingle, J.D. (1988), *Spectrochemical Analysis,* Prentice-Hall, Inc., Engelwood Cliffs, New Jersey, pp. 424-425.

Jakubauskas, M.E., 1996, "Thematic Mapper Characterization of Lodgepole Pine Seral Stages in Yellowstone National Park, USA," *Remote Sensing of Environment*, **56**:118-132.

Kokaly, R.F., Despain, D.G., Clark, R.N., and Livo, K.E. (2001) "Spectral feature analysis for mapping vegetation cover and microbial communities in Yellowstone National Park using AVIRIS," submitted to *Remote Sensing of Environment.*

Kokaly, R.F. and Clark, R.N. (1999), Spectroscopic determination of leaf biochemistry using band-depth analysis of absorption features and stepwise multiple linear regression. *Remote Sensing of Environment* **67:** 267-287.

Kokaly, R.F., Clark, R.N., and Livo, K.E. (1998) "Mapping the Biology and Mineralogy of Yellowstone National Park using Imaging Spectroscopy," *Summaries of the 7th Annual JPL Airborne Earth Science Workshop, January12-16, 1998, Volume 1. AVIRIS Workshop,* R.O. Green, Ed., JPL Publication 97-21, pp. 245-254.

Martin, M.E., Newman, S.D., Aber, J.D., and Congalton, R.G., 1998, "Determining forest species composition using high spectral resolution remote sensing data," *Remote Sensing of Environment*, vol. **65**:249-254.

Martin, M.E., and Aber, J.D. (1997), High spectral resolution remote sensing of forest canopy lignin, nitrogen, and ecosystem processes. *Ecological Applications* **7**:431-443.

Mustard, J.F., Staid, M.L., and Fripp, W. (1999) "Atmospheric correction and inverse modeling of AVIRIS data to obtain water constituent abundances," *Summaries of the 8th JPL Airborne Earth Science Workshop*, R.O. Green, Ed., JPL Publication 99-17, pp. 309-315.

Roberts, D.A., Gardner, M., Church, R., Ustin, S., Scheer, G., and Green, R.O., 1998, "Mapping chaparral in the Santa Monica Mountains using multiple endmember spectral mixture models," *Remote Sensing of Environment*, **65**:267-279.

Ustin, S.L., Smith, M.O., Jacquemoud, S., Verstraete, M., and Govaerts, Y. (1999), Geobotany: Vegetation mapping in earth sciences. In *Remote Sensing for the Earth Sciences: Manual of Remote Sensing 3rd Edition, Vol. 3* (A.N. Rencz Ed.), John Wiley and Sons, Inc., New York, pp. 189-248.

Wessman, C.A., Aber, J.D., and Peterson, D.L. (1989), An evaluation of imaging spectrometry for estimating forest canopy chemistry, *International Journal of Remote Sensing* **10**:1293-1316.

Table 1. AVIRIS Data Collection Parameters for High and Low Altitude Acquisitions.

Parameter	High Altitude	Low Altitude
Date	August 7, 1996	October 13, 1998
Time (local)	10:32 am	10:43 am
Platform	NASA ER-2	NOAA Twin Otter
Aircraft Altitude (km)	20.0	3.81
Solar Azimuth (degrees)	139.6	154.4
Solar Elevation (degrees)	44.3	34.3
Nominal pixel size (m)	17.5	1.5
Ground Sampling Distance (m) Cross-track (near nadir)	15.4	1.3

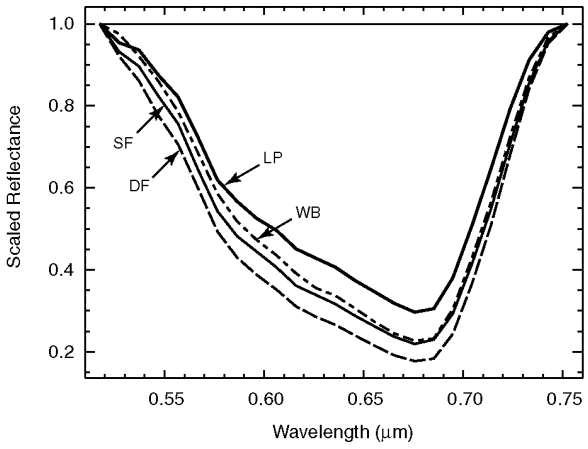

Figure 1. Continuum removed chlorophyll absorption feature of conifer vegetation cover types occurring in Yellowstone National Park (lodgepole pine, LP; Douglas-fir, DF; whitebark pine, WB; and mixed Engelmann spruce/subalpine fir, SF)

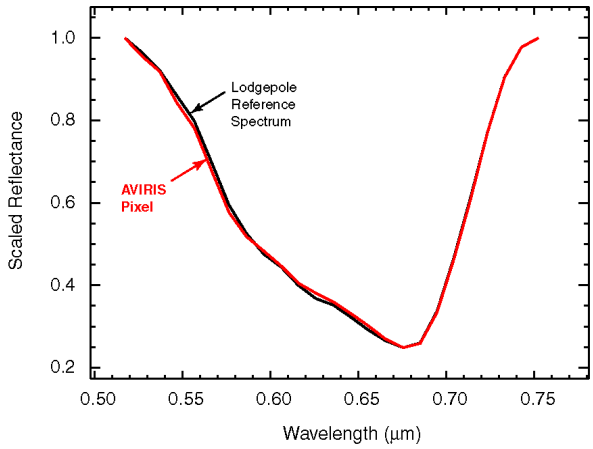

Figure 2. A comparison of the continuum removed and scaled absorption features of the spectrum of an AVIRIS pixel and the vegetation cover type (lodgepole pine) identified by the USGS Tetracorder expert system as the best match.

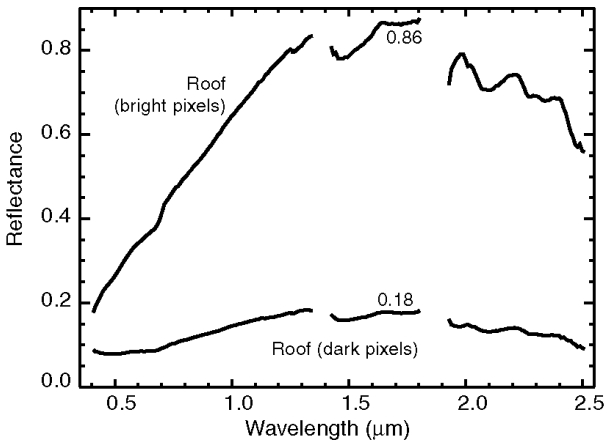

Figure 3. The average AVIRIS 1998 low altitude reflectance spectra for two sides of a pitched roof in the Old Faithful area (Figure 4a). The reflectance value at 1.7 μm is given.

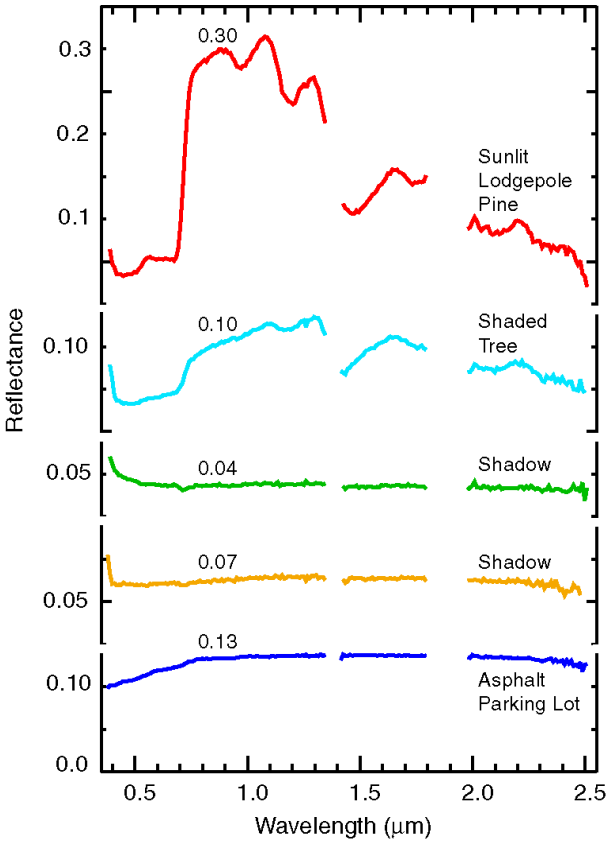

Figure 4. Reflectance spectra of sunlit tree, shaded tree, shaded parking lot, and sunlit parking lot from the AVIRIS 1998 low altitude data.

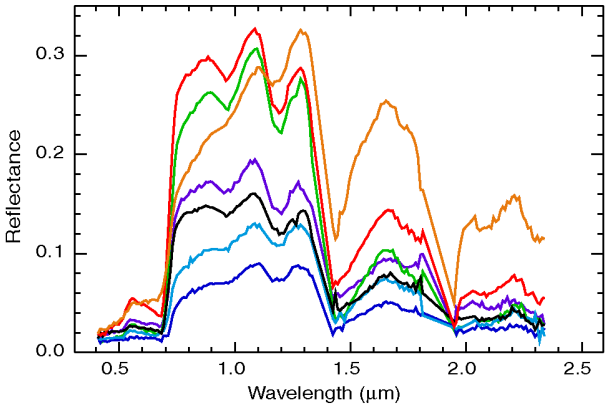

Figure 5. Reflectance spectra of pixels extracted from an area of lodgepole pine just north of Old Faithful geyser.

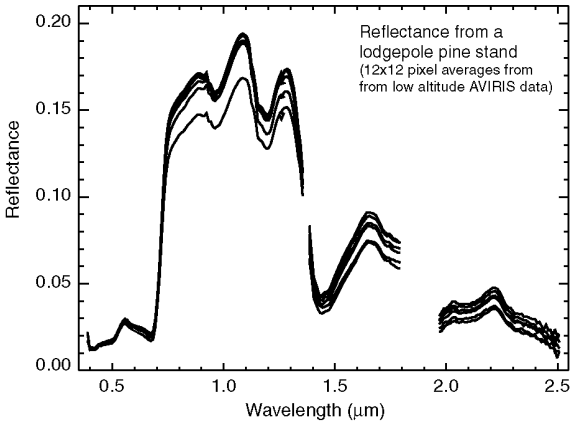

Figure 6. Reflectance spectra of low altitude data averaged in 12x12 blocks for an area of lodgepole pine just north of Old Faithful geyser, which show less variation in their reflectance signatures compared to individual pixels as depicted in Figure 5.

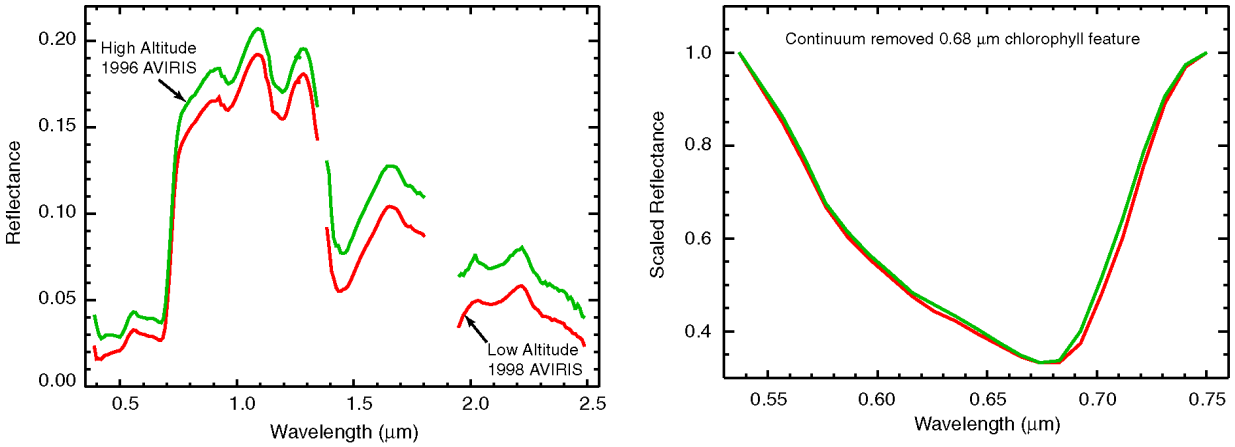

Figure 7. A comparison of the averaged reflectance signatures of the lodgepole pine stand just north of Old Faithful geyser (Figure 7a) and their 0.68 µm chlorophyll absorption feature that has been continuum removed and scaled (Figure 7b)

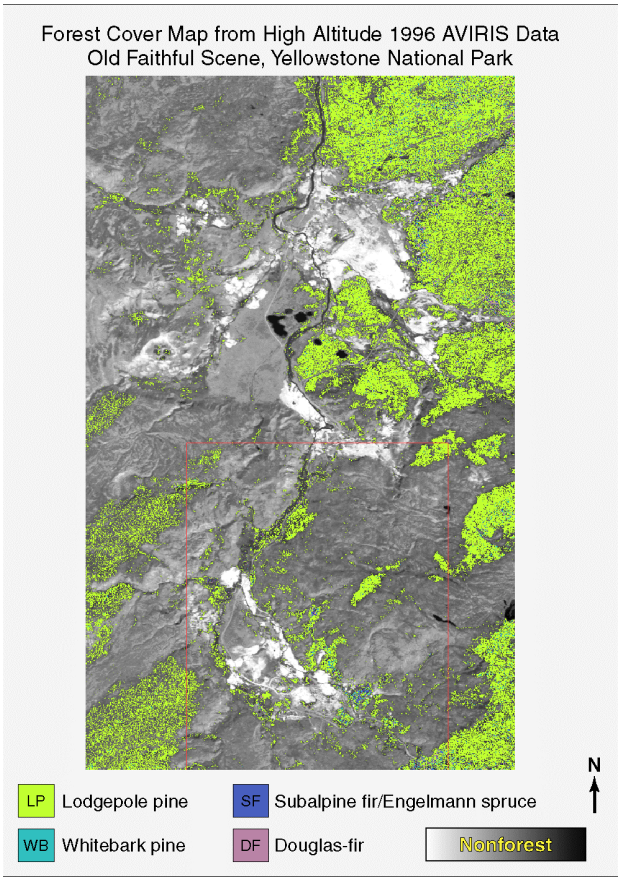

Figure 8. Forest cover map of a 1024 line scene of high altitude 1996 AVIRIS data over the Old Faithful area generated using the USGS Tetracorder expert system.

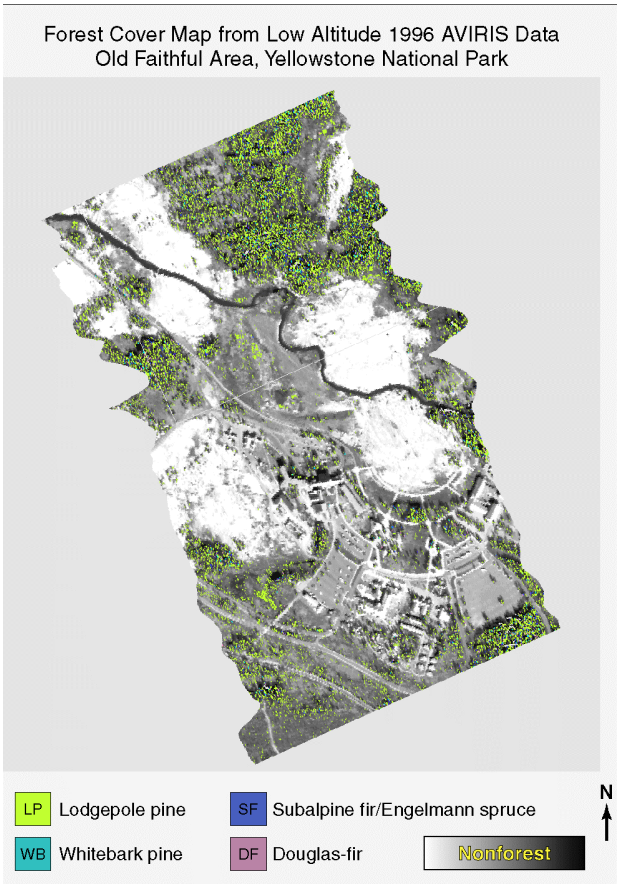

Figure 9. Forest cover map of a 1024 line scene of low altitude 1998 AVIRIS data over the Old Faithful area generated using the USGS Tetracorder expert system.

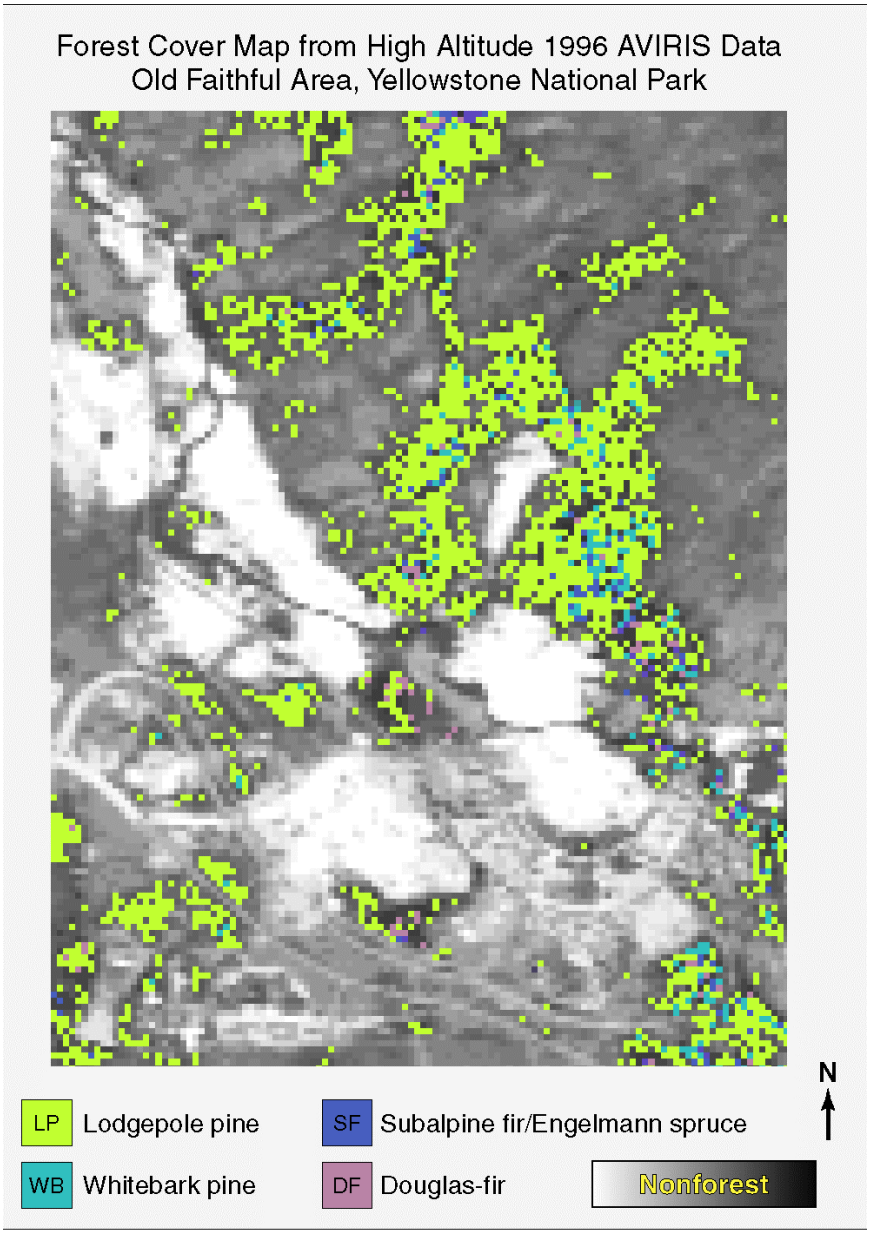

Figure 10. Forest cover map of the Old Faithful area taken from a scene of high altitude 1996 AVIRIS data over the Old Faithful generated using the USGS Tetracorder expert system.